Effect of Glass Frit Chemistry on the Physical and Electrical Properties of Thick-Film Ag Contacts for Silicon Solar Cells

MOHAMED M. HILALI,[1,4] SRINIVASAN SRIDHARAN,[2] CHANDRA KHADILKAR,[2] AZIZ SHAIKH,[3] AJEET ROHATGI,[1] and STEVE KIM[3]

1.—School of Electrical and Computer Engineering, Georgia Institute of Technology, Atlanta, GA 30332-0250. 2.—Ferro Corporation, Technical Center, 7500 E. Pleasant Valley Rd., Independence, OH 44131. 3.—Ferro Corporation, 1395 Aspen Way, Vista, CA 92083. 4.—E-mail: mhilali@adventsolar.com

The aim of this study is to understand the effect of the glass frit chemistry used in thick-film Ag pastes on the electrical performance of the silicon solar cell. The study focuses on the physical behavior of the glass frit during heat treatment as well as the resulting Ag-Si contact interface structure. We observe that the glass frit transition temperature (T_g) and softening characteristics play a critical role in the contact interface structure. The glass transition temperature also significantly influences the contact ohmicity of the thick-film metal grid. A high glass frit transition temperature generally results in thinner glass regions between the Ag bulk of the grid and the Si emitter. It was found that a glass frit (with high T_g) that crystallizes fast during the firing cycle after etching the silicon nitride and Si emitter results in smaller Ag crystallite precipitation at the contact interface. This results in smaller junction leakage current density (J_{o2}) and higher open-circuit voltage (V_{oc}). Using high T_g pastes (with the appropriate Ag powder size), greater than 0.78 fill factors and >17.4% efficiency were achieved on 4 cm^2 untextured single crystal Si solar cells with 100 Ω/sq emitters.

Key words: Si solar cells, screen-printing, thick-film contacts, glass frit, glass transition temperature

INTRODUCTION

The glass frit in Ag pastes plays a critical role in the screen-printed metallization process for industrial silicon solar cells. For subeutectic screen-printed contact formation, the glass frit is obviously a crucial factor for good-quality Ag-Si ohmic contacts as it is necessary to punch through the antireflection coating (ARC) and because it plays a very important role in the contact formation mechanism.[1] The glass frit is a binder phase, which dissolves the metal powder and sticks to the substrate or provides adhesion during high-temperature firing. It also affects the metal powder sintering kinetics. It is a mixture of metal oxides and silicon dioxide melted to form a uniform glass. Before being added to the paste, the glass is milled to a thin sheet and crushed. Normally, lead oxide glass is the most important ingredient, which is added in amounts of ~1–5%. Other additives or modifiers can be added, such as bismuth, aluminum, titanium, and zinc.

Phosphorus can also be added to improve contact to the n$^+$-type emitter. The glass frit in the Ag paste is the main factor that determines the contact resistance, silicon surface etching, and ultimately the overall surface performance. It is required for good electrical and mechanical performance (adhesion and forming a bond in the thick-film). Nevertheless, the type and amount of glass frit is responsible for open-circuit voltage and fill factor degradation at higher paste firing temperatures.

Figure 1 illustrates the structure of the conventional silicon solar cell fabricated in this study. The conventional silicon solar cell has a p-type substrate, an n$^+$ front phosphorus emitter, a front metal-grid printed on top of a passivating and antireflection film (typically silicon nitride), an aluminum back contact and a p$^+$ back-surface field (BSF) that forms during the metal contact firing step where the aluminum alloys with the Si. During the metal-contact firing step of the solar cell fabrication process, the glass frit in the Ag front grid paste, typically composed of lead borosilicate glass, etches through the SiN$_x$ ARC and provides contact

adhesion to the underlying silicon.[2] Complete etching of the SiN_x ARC is necessary for the formation of good ohmic contacts. At temperatures greater than 600°C, the glass frit fluidizes and wets the silicon nitride antireflection coating surface. The liquid glass frit starts dissolving the Ag particles upon contact. As the temperature rises, the glass frit starts to etch the silicon nitride film. The etching by the glass takes place via a redox reaction.[3] Upon full penetration of the silicon nitride film, the Si emitter surface starts dissolving in the liquid glass. Moreover, the liquid glass frit acts as a medium for Ag transport to the Si emitter surface. During the cooling stage of the firing, Ag and Pb separate according to their phase diagram, and Ag precipitates as crystallites (inverted pyramids) on the Si emitter surface.[4] Lead precipitates as granules in the glass layer. The ohmic contact for screen-printed metallization is achieved by metallic elements coming from the oxide glasses.[5] This was supported by Ballif who showed that Ag crystallites that supersaturate from the glass layer during cooling achieve very low contact resistivity.[6]

The viscosity of the glass is one of the most important properties that define the glass behavior.[7] Therefore, this study is focused on the glass softening and flow characteristics during the metal thick-film contact firing cycle. In this paper, we will make an attempt to understand how to control the contact quality by tailoring the key constituents of the paste such as the glass transition temperature and crystallization behavior.

EXPERIMENTAL

In this study, many screen-printed cells were fabricated by cofiring the contacts either at a conventional temperature of $\geq 750°C$ or at a higher temperature of $\geq 840°C$ for several carefully formulated pastes with different chemistry. It is challenging to measure the exact temperature of the wafer in a belt furnace with rapid belt speed. An attempt was made to measure the wafer peak temperature by a K-type thermocouple attached to a companion cell traveling through the belt furnace. There could be some error in the measured peak temperature due to the thermocouple response time and bonding. Table I shows the formulation of four different pastes studied. These pastes have different glass frit chemistry to control the glass transition temperature (T_g) (below which the glass frit becomes hard and brittle) and aggressiveness (responsible for etching of the SiN_x and Si layers). For the glass frits investigated in this paper, the T_g and glass softening point (where the glass starts to flow by its own weight) ranged from ~400°C to 600°C. The substrates were (100) planar float zone (FZ) Si wafers, which received $H_2SO_4 : H_2O_2 : H_2O$ (1:1:2) followed by $HCl : H_2O_2 : H_2O$ (1:1:2) cleaning solutions with $HF : DI$ water (1:10) solution and DI water rinse at the beginning and at the end of the cleaning sequence and between each cleaning solution. This
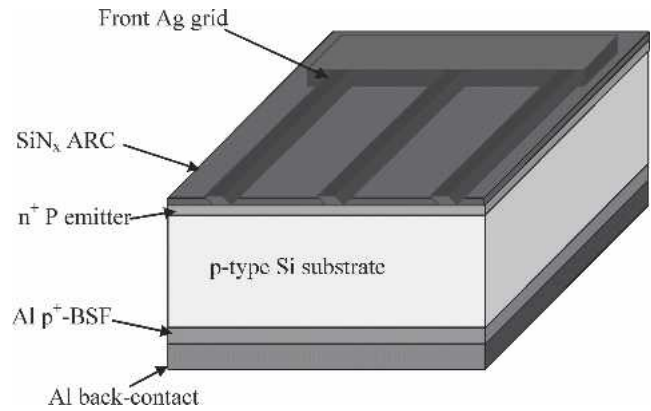

Fig. 1. Si solar cell diagram.

Table I. Glass Properties for each Ag Paste.

Paste/Glass Type	Glass Frit Properties	Ag Powder Size
33-460/GF1	lowest T_g, less aggressive	Blend
33-452/GF2	medium T_g, more aggressive	Blend
33-462/GF3	medium-high T_g, more aggressive	Blend
33-455/GF4	high T_g, less aggressive	Blend
A203-7B/GF4	high T_g, less aggressive	Medium
A203-7A/GF4	high T_g, less aggressive	Large

[a]Blend indicates a blend of small and medium Ag particle sizes.

was followed by $POCl_3$ diffusion to form an n^+ 100 Ω/sq emitter. The emitter was formed by one-step $POCl_3$ diffusion. After the phosphorus-glass removal and another cleaning step, 50 KHz plasma-enhanced chemical vapor deposition (PECVD) SiN_x antireflection coating was deposited on the emitter. Next, an Al paste was screen-printed on the backside and dried at 200°C. The Ag grid was then screen-printed on top of the SiN_x film, and the Ag and Al contacts were cofired (single firing step) in a lamp-heated three-zone infrared belt furnace. The cells were then annealed in forming-gas at 400°C for ~15 min. I-V analysis was used to determine cell performance and fill factor (FF). The transfer-length method[8] (TLM) measurements were used for obtaining specific contact resistance. The Suns-V_{oc} technique[9] was used for measuring the junction-leakage current.

RESULTS AND DISCUSSION

Effect of Glass Transition Temperature on the Contact Behavior for Different Firing Temperatures and Belt Speed

The glass transition temperature (T_g) was varied to see how it affects the contacts. It is important to realize that a lower T_g glass with low softening

Effect of Glass Frit Chemistry on the Physical and
Electrical Properties of Thick-Film Ag Contacts
for Silicon Solar Cells

2043

point starts to fluidize at lower temperatures and can increase the thickness of the glass. The effect of glass frit in the Ag paste was studied for different firing schemes to understand the interaction of frit chemistry and firing temperature. First, the effect of ~840°C firing at a belt speed of 80 ipm on high (90–95 Ω/sq) and low (40–45 Ω/sq) sheet-resistance emitters was studied (Fig. 2). On the high sheet-resistance emitter, paste 33-455 with lower Pb content in the glass and a higher T_g gave a FF of less than 0.70 because of high series resistance (2.6 Ω cm^2) and somewhat high specific contact resistance ρ_{cm} (7.5 mΩ cm^2). Specific contact resistance below 3 mΩ cm^2 is generally acceptable. The same high T_g paste gave R_s of ~0.643 Ω cm^2 on the 40 Ω/sq emitter. Pastes 33-452 and 33-462, which have slightly lower glass transition temperatures and different glass frit viscosity behavior, gave acceptably low macroscopic specific contact resistance (0.35–1 mΩ cm^2) on the 90–95 Ω/sq emitter.

Next, the use of conventional (750°C) firing with faster belt speed was compared to $\geq$840°C firing. Figure 3 shows that high FFs were achieved on 100 Ω/sq emitters at $\geq$840°C with 120 ipm belt speed for all three pastes. However, at $\geq$750°C firing, high FF
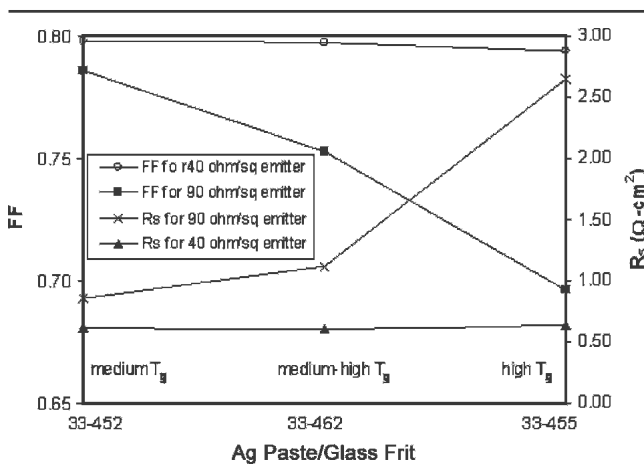

Fig. 2. Response of Ag pastes with different glass frit T_g on 90–95 Ω/sq and 40 Ω/sq emitters fired at ~840°C/80 ipm.
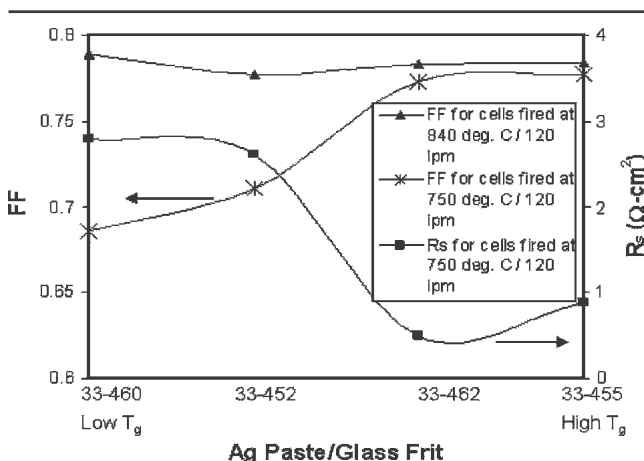

Fig. 3. Effect of glass frit chemistry and firing temperature on the series resistance and FF of solar cells.

was achieved only for medium-high and high T_g glass Ag pastes (33-462 and 33-455). This demonstrates that, unlike the case with the PV168 Ag paste,[10,11] a high firing temperature of $\geq$835°C is not always necessary to achieve a good ohmic contact to the 100 Ω/sq emitter, provided high T_g glass and fast belt speed are used. However, lower T_g glass frits GF1 (33-460) and GF2 (33-452) gave significantly lower FFs for the 750°C firing. Figure 3 shows that this is primarily due to higher series resistance resulting from higher macroscopic specific contact resistance. Thus, the glass frit chemistry dictates whether good ohmic contacts can be achieved at the desired firing temperature. Paste 33-460, which has a low T_g glass and is less aggressive, gave poor FFs (0.686) at lower-temperature firing. However, for the $\geq$840°C firing, paste 33-460 gave excellent FFs of 0.789. Paste 33-452, which also has a lower T_g compared to paste 33-455, gave a lower FF of 0.710 at $\geq$750°C firing temperature, which increased to ~0.777 at 840°C firing (Fig. 3). This increase in FF was reflected in a decrease in ρ_{cm} from 9.07 mΩ cm^2 to 1.09 mΩ cm^2. The highest fill factors were achieved with the higher T_g pastes 33-462 and 33-455 due to the low series resistance. Paste 33-455, which has a higher T_g (less fluid) and is less aggressive, also showed a slight improvement in FF, from ~0.777 to ~0.783 when going from the $\geq$750°C at 120 ipm to the $\geq$840°C at 120 ipm condition after forming gas anneal. The combined effect of glass T_g, firing temperature, and belt speed can be summarized as follows:

- Lower T_g glass gives high FFs at $\geq$840°C for both faster (120 ipm) and slow (80 ipm) belt speeds in spite of it resulting in a thick glass layer. The high-temperature firing followed by forming gas anneal (FGA) probably results in the formation of more metal precipitates in the glass to promote multistep tunneling through the thick glass.
- High T_g (less fluid) glass gives high FFs only at faster belt speeds (for both $\geq$750°C and $\geq$840°C firing temperatures) because high T_g and faster belt speed help the formation of thin glass regions, which facilitates tunneling.
- For conventional firing conditions ($\geq$750°C/120 ipm) the pastes that have higher T_g glass give good FFs. The low T_g glass (GF1 of paste 33-460) does not work well with conventional (700–790°C) firing temperature, even with fast belt speed, because the glass layer is always too thick due to the high fluidity of the glass and probably because there are not enough metal precipitates in the glass for effective tunneling.

Metal precipitates in the glass are observed only in over-fired (e.g., $\geq$840°C) samples.[6] For the lower T_g glass frits (GF1 and GF2) fired at ~750°C with 120 ipm belt speed, there are not enough metal precipitates in the glass layer to assist the current transport. Therefore, carrier transport takes place primarily via tunneling through ultrathin glass regions between the Ag crystallites and the bulk Ag. In this case, FGA does not play an important

role. Instead the thickness of the glass layer becomes more important for current transport.

The above study shows that the combination of glass frit T_g and the firing process plays an important role in achieving good contact to high sheet-resistance emitters because it dictates the thickness and conductivity of the glass layer, Ag precipitates, and multistep tunneling.[12]

To further understand the effect of T_g on the contact formation, scanning electron microscope (SEM) images were obtained for the three glass frit types (GF1, GF2, and GF4). As expected, Fig. 4 shows that the glass frit with lower T_g (GF1) gave a thicker glass layer compared to the higher T_g glass frit (GF4). The images in Fig. 4 are generally representative of different cross-sections of the contact interface for the different pastes. Thinner glass layers should result in lower contact resistance[12–14] because of the higher tunneling probability. Faster
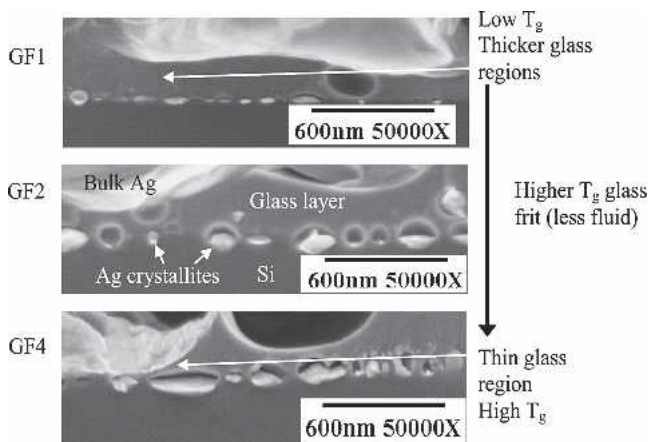
firing tends to give thinner glass regions by reducing the time for the glass layer to seep to the Si surface.

Figure 5 shows that the low T_g glass frit (paste 33-460) also results in larger and more frequent distribution of Ag crystallites compared with the higher T_g glass frit (paste 33-462). This is because the lower the glass T_g, the earlier the glass starts to flow during the firing cycle. This allows the glass to interact with the Ag particles for a longer period of time during firing. This dissolves more Ag before it completely sinters, resulting in a greater number of Ag crystallite precipitates. The lower T_g glass is thicker after firing because it is more fluid, so less of it is retained within the bulk of the Ag grid.

Formulation and Investigation of a Novel Fast-Crystallizing Glass Frit with High T_g

The previous section showed that low T_g glass tends to give a thicker glass layer and a higher frequency of larger Ag crystallites. Large Ag crystallites could cause junction shunting in shallow emitters. They could also lead to a higher emitter saturation current density because of the larger metal-contact area. Thin glass layers are desirable for tunneling. Therefore, a large number of very small Ag crystallites in conjunction with thin glass regions is most suitable for shallow emitters. Based on the above understanding, a new commercial Ag paste (33-455) was formulated that not only has high T_g glass but also crystallizes rapidly after reaching a high temperature. Thin glass regions are observed at the contact interface. In addition, rapid crystallization of the glass at higher temperatures "freezes" the glass early so Ag crystallites are not allowed to fully precipitate from the glass. As a result, smaller Ag crystallites and less Ag diffusion into the siemitter are achieved, which reduces
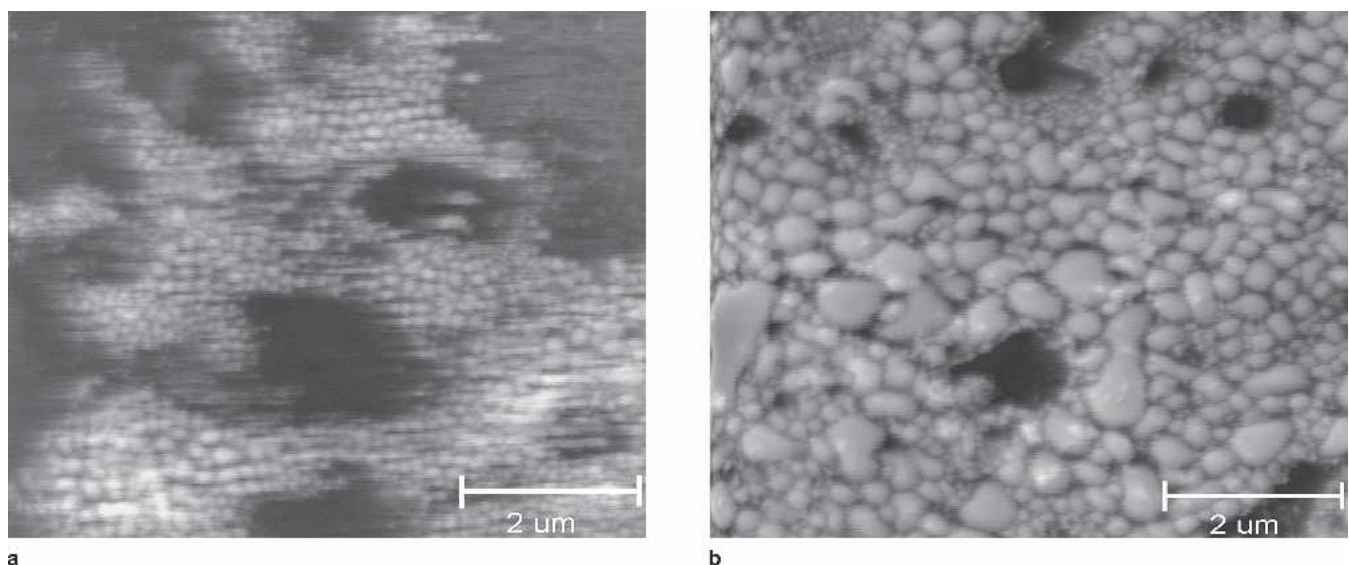

Fig. 4. SEM images showing the effect of glass T_g on the Ag-Si contact interface.

a											b

Fig. 5. SEM top-view images of the contact interface for (a) higher-T_g glass (33-462) and (b) lowest-T_g glass of paste 33-460. The images show Ag precipitates on the Si emitter surface. The glass frit and bulk Ag were selectively etched-off before taking the images using a sequence of hot nitric acid for etching the bulk Ag, followed by hydrofluoric acid solution for etching the glass frit.

Effect of Glass Frit Chemistry on the Physical and
Electrical Properties of Thick-Film Ag Contacts
for Silicon Solar Cells

2045

the probability of junction shunting for shallow emitters. In addition, more Ag precipitates within the glass could help in metal assisted tunneling through the glass layer. Thus, this paste should have most of the ingredients for good contacts. The new paste (33-455) was formulated by adding some modifiers that provide nucleation sites to promote early crystallization near the peak temperature during firing, just before or after the cooling starts. Solar cells were fabricated and analyzed by electrical and physical characterization tools to understand the contact interface and its correlation with the contact and cell performance.

SEM cross sections of the contact interface in Fig. 6 show that paste 33-455 with rapidly crystallizing frit has smaller Ag precipitates on the Si emitter surface (Fig. 6a) compared with paste 33-462 with conventional frit (Fig. 6b). Cell analysis revealed
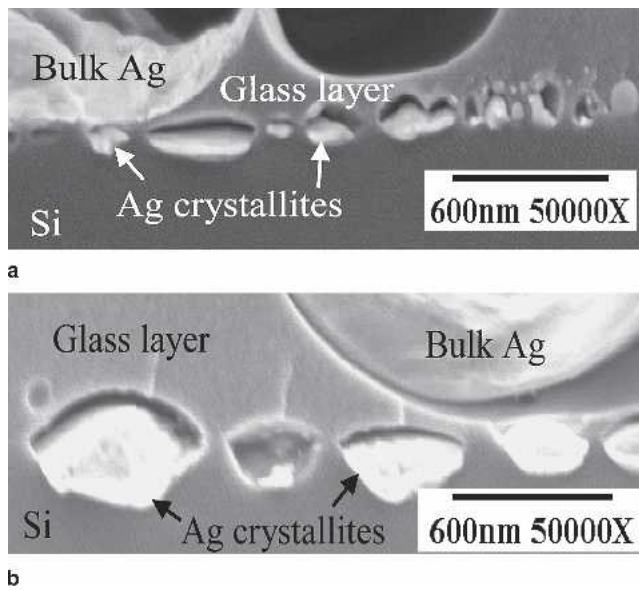

Fig. 6. SEM cross-section images of the Ag-Si contact interface for (a) high T_g fast-crystallizing glass (paste 33-455), and (b) conventional glass (paste 33-462).

lower junction leakage current, J_{o2} of 12 nA/cm^2, and a higher V_{oc} of ~645 mV for paste 33-455 compared to J_{o2} of ~25 nA/cm^2 and V_{oc} of ~640 mV for the conventional glass paste 33-462, where larger Ag crystallites contributed to the higher J_{o2}.

To further prove the concept that the rapidly crystallizing glass frit in paste 33-455 gave higher FF and V_{oc} by decreasing the size of Ag crystallites, another fast-crystallizing glass paste (A203-7A) was formed with large Ag particles. It has been shown that for a paste with such large Ag particles, high junction leakage degrades the V_{oc} and FF.[15] However, by converting it into a rapid-crystallization paste, reduction of the Ag crystallite size was achieved in conjunction with higher FF and V_{oc}, resulting in ~0.5% increase in absolute cell efficiency. The enhancement in V_{oc} and efficiency for the medium and large particle size pastes, resulting from the transformation to fast-crystallizing glass frit, is shown in Fig. 7. Detailed cell analysis showed that this enhancement in V_{oc} is mainly due to a decrease in J_{oe} from ~500 fA/cm^2 to ~320 fA/cm^2, probably because of the reduced metal coverage due to the smaller Ag crystallites. J_{o2} also decreased from ~35 nA/cm^2 to ~15 nA/cm^2 as a result of the decrease in the size of Ag crystallites. Figure 8 shows the cross-sectional SEM of the two interfaces formed with (a) paste with medium-size Ag particles and a fast-crystallizing glass frit (A203-7B) and (b) paste (33-462) with conventional glass frit and mostly medium Ag particle size. Notice that the conventional glass frit results in generally larger Ag crystallites at the contact interface, which could degrade a shallow junction.

Fabrication of High-Efficiency Cells on 100 Ω/sq Planar Emitters

Consistent with our understanding and analysis of the contact interface in the previous sections, attempts were made in this section to achieve high-efficiency cells using the two most desirable
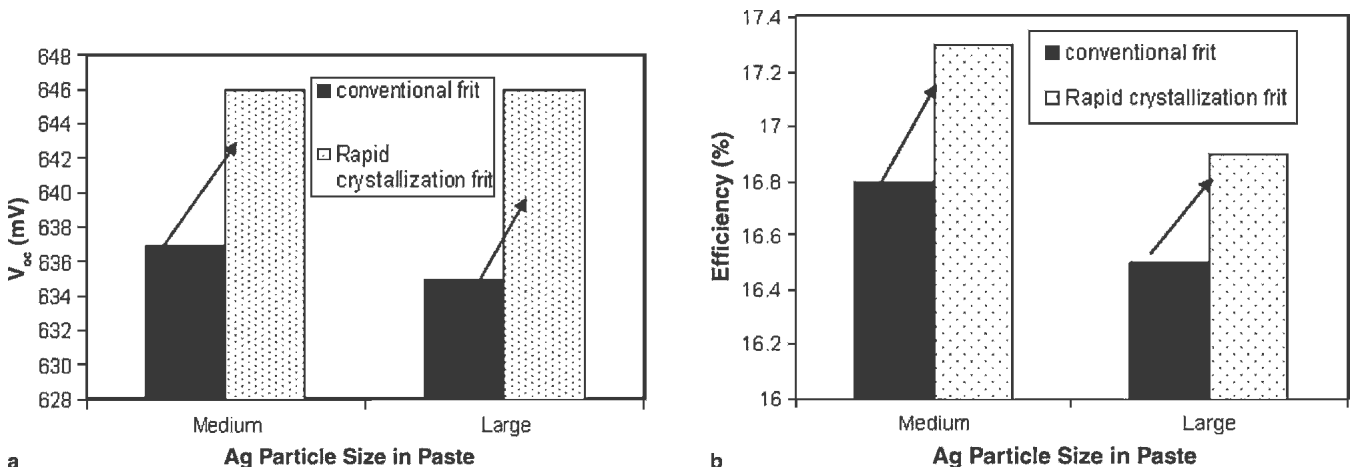

Fig. 7. Enhancement in (a) V_{oc} and (b) efficiency for the medium (paste A203-7B) and large (paste A203-7A) Ag particle size pastes with a rapid-crystallizing glass frit compared to medium and large Ag particle size pastes with conventional glass frit.

pastes: 33-462 and 33-455 for high sheet-resistance shallow emitters. Figure 9 shows that untextured FZ cell efficiencies as high as 17.4% on 100 Ω/sq emitters were achieved, although there was some scatter or nonuniformity in the performance of >50 cells made with the 100 Ω/sq emitter. Fill factors are generally high for the 40 Ω/sq-emitter cells because of the lower sheet-resistance loss. However, when a good ohmic contact is achieved on 90–100 Ω/sq emitters with a good surface passivation, a clear improvement of ~0.2–0.4% in absolute efficiency was observed over the ~40 Ω/sq emitter.
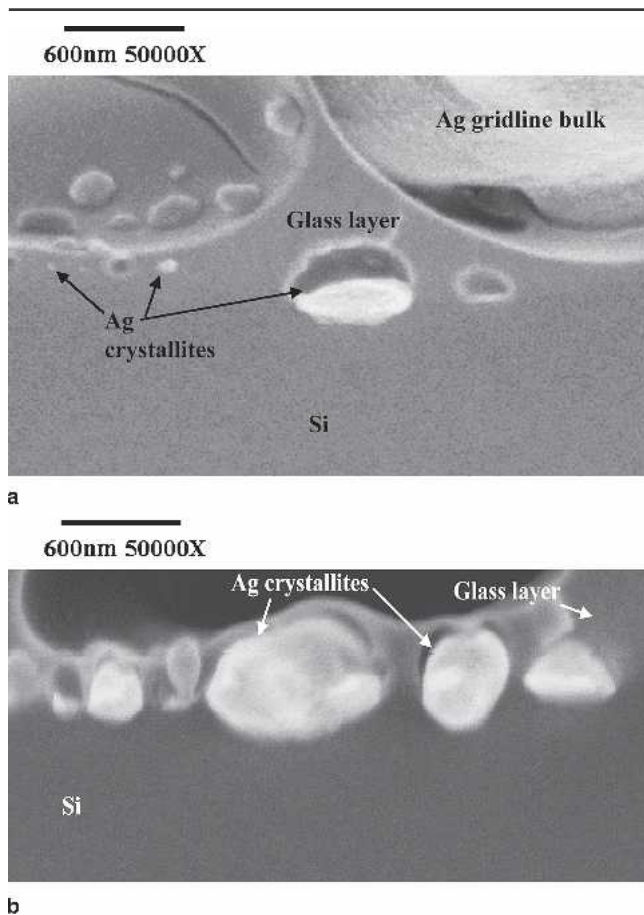

Fig. 8. SEM cross-section images of the Ag-Si contact interface for medium particle-size pastes: (a) fast-crystallizing glass (paste A203-7B) and (b) conventional glass frit (33-462).
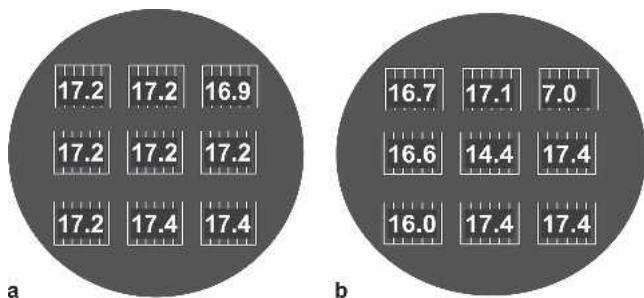

Fig. 9. The efficiency distribution of nine 4 cm² cells on a 4 in FZ Si wafer on a 100 Ω/sq emitter using paste 33-455 fired at (a) 840°C/120 ipm and (b) 750°C/120 ipm.

Tables II and III show the best and average cell efficiencies achieved on 100 and 40 Ω/sq emitters using commercially available Ag paste 33-462. Figure 9 shows the best spatial distribution for the nine 4 cm² cells on a 4 in. diameter FZ wafer. This was obtained using the commercially available Ag paste 33-455 and a firing condition of 840°C/120 ipm, followed by forming gas anneal (FGA). These cells had an average FF of 0.779 and an average efficiency of 17.2%. Figure 9b shows that for paste 33-455 with rapidly crystallizing glass, high-efficiency cells were achieved with ~750°C firing conditions. It is also important to note that the paste 33-455 had a lower lead content (~40% lower) than the other pastes, which is good for the environment.

CONCLUSIONS

The glass frit chemistry was altered in the paste by changing its glass transition temperature and aggressiveness. It was found that low T_g glass softens early, dissolves more Ag, and flows more easily to form a thicker glass layer. Also, there are probably not enough metal precipitates in the thick glass layer to aid multistep tunneling for conventional contact firing temperatures. A glass frit with a high T_g (less fluid) makes better contact with the Si emitter under conventional firing conditions (750°C/120 ipm). A glass frit with a low-medium (more fluid) T_g appears to be less sensitive to firing time. The glass frit primarily determines the optimum firing temperature needed to make good ohmic contacts. A fast-crystallizing glass with high T_g was demonstrated to be better, reducing the crystallite size and enhancing the V_{oc} and cell efficiency because of reduced shunting, junction leakage, and reduced emitter saturation current density. Even though low T_g glass did not work well at the lower firing temperature (~750°C), it gave good contact and high FF at higher firing temperatures of ~840°C in conjunction with a 400°C forming gas anneal. This is attributed to the presence of more metal precipitates in the glass layer to promote multistep tunneling. Higher belt speed (rapid firing) was found to be important for higher T_g glass frit to prevent the formation of generally thick glass regions at the Ag-Si contact interface. Based on the understanding of the particle size and frit chemistry, a novel paste was formulated that had a blend of small-medium Ag particles, high T_g glass, and modifiers to nucleate rapid crystallization at higher temperatures. This reduced the Ag crystallite size to prevent high junction leakage and shunting of shallow emitters and probably increased the metal precipitation within the glass layer to help metal-assisted multistep tunneling. This paste also resulted in low specific contact resistance values due to the high T_g of the glass frit. All these features contributed to a high FF of 0.783 on 100 Ω/sq emitter resulting in planar cell efficiencies as high as 17.4%. This represents about a 0.4% increase in absolute efficiency over the conventional 40 Ω/sq emitter cells.

Effect of Glass Frit Chemistry on the Physical and
Electrical Properties of Thick-Film Ag Contacts
for Silicon Solar Cells

2047

Table II. 90–100 Ω/sq-Emitter Cells Using Paste 33-462

Cell Name	V_{oc}(mV)	J_{sc}(mA/cm^2)	FF	Eff(%)	n factor	R_s(Ω cm^2)	R_{sh}(Ω cm^2)
Best Cell	642	34.31	0.786	17.32	1.03	0.948	27725
Average	640	34.34	0.773	17.00	1.12	0.553	233546
Standard Dev.	1	0.16	0.009	0.23	0.03	0.162	599234

Table III. 40 Ω/sq-Emitter Cells Using Paste 33-462

Cell Name	V_{oc}(mV)	J_{sc}(mA/cm^2)	FF	Eff(%)	n factor	R_s(Ω cm^2)	R_{sh}(Ω cm^2)
Best Cell	638	33.66	0.797	17.1	1.03	0.592	94677
Average	637	33.50	0.790	16.87	1.05	0.719	50409
Standard Dev.	1	0.13	0.010	0.22	0.02	0.168	79500

ACKNOWLEDGEMENTS

REFERENCES

1. G. Schubert, F. Huster, and P. Fath, *Proc. 19th European Photovoltaic Solar Energy Conference* (Munich, Germany: WIP-Munich and Florence, Italy: ETA Florence, 2004), pp. 813–816.
2. J. Hoornstra, G. Schubert, and K. Broek, *Proc. 31st IEEE Photovoltaic Specialists Conference* (Piscataway, NJ: IEEE, 2005), pp. 1293–1296.
3. R.J.S. Young and A.F. Carroll, *Proc. 16th European Photovoltaic Energy Conference*, Vol. II (London: James & James Science Publishers, 2000), pp. 1731–1734.
4. C. Ballif, D.M. Huljić, A. Hessler-Wysser, and G. Willeke, *Proc. 29th IEEE Photovoltaic Specialists Conference* (Piscataway, NJ, IEEE, 2002), pp. 360–363.
5. B. Thuillier, S. Berger, J.P. Boyeaux, and A. Laugier, *Proc. 28th IEEE Photovoltaic Specialists Conference* (Piscataway, NJ: IEEE, 2000), pp. 411–413.
6. C. Ballif, D.M. Huljić, G. Willeke, and A. Hessler-Wysser, *Appl. Phys. Lett.* 82, 1878 (2003).
7. A.K. Varshneya and T.P. Seward III, *Handbook of Ceramics, Glasses, and Diamonds,* ed. C.A. Harper (New York: McGraw-Hill, 2001), Chap. 5, p. 33.
8. D.K. Schroder, *Semiconductor Material and Device Characterization* (New York: John Wiley & Sons, 1990), p. 119.
9. R.A. Sinton and A. Cuevas, *Proc. 16th European Photovoltaic Solar Energy Conference,* Vol. II, Glasgow, UK (London: James & James Science Publishers, 2000), pp. 1152–1155.
10. M.M. Hilali, M.M. Al-Jassim, B. To, H. Moutinho, A. Rohatgi, and S. Asher, *J. Electrochem. Soc.* 152, G742 (2005).
11. M.M. Hilali, A. Rohatgi, and S. Asher, *IEEE Trans. Electron. Dev.* 51, 948 (2004).
12. C. Khadilkar, S. Kim, T. Pham, A. Shaikh, and S. Sridharan, Technical Digest of the 14th International Photovoltaic Science and Engineering Conference (Bangkok, Thailand: Chulalongkorn University, 2004), pp. 443–444.
13. A. Shaikh, S. Sridharan, T. Pham, and C. Khadilkar, *Proc. 3rd World Conference on Photovoltaic Energy Conversion* (Japan, World Conference on Photoroltaic Energy Conversion (WCPEC), 2003), pp. 1500–1503.
14. S. Sridharan, C. Khadilkar, T. Pham, and A. Shaikh, *Proc. 13th Workshop on Crystalline Silicon Solar Cell Materials and Processes* (Golden, CO: National Renewable Energy Lab (NREL), 2003), pp. 162–165.
15. M.M. Hilali, K. Nakayashiki, C. Khadilkar, R.C. Reedy, A. Rohatgi, A. Shaikh, S. Kim, and S. Sridharan, *J. Electrochem. Soc.* 153, A5 (2006).